Charge, strangeness and radius of strangelets

X. J. Wen,[1,2,3] G. X. Peng,[1,2,3*] Y. D. Chen,[2,3]

[1]*China Center of Advanced Science and Technology (World Lab.), Beijing 100080, China*
[2]*Institute of High Energy Physics, Chinese Academy of Sciences, Beijing 100049, China*
[3]*Graduate University of Chinese Academy of Sciences, Beijing 100049, China*

February 1, 2008

Abstract

We investigate, at both zero and finite temperature, the properties of strangelets versus the electric charge Z and strangeness S. The strangelet radius is not a monotonic function of either charge or strangeness, and a minimum is reached in the (Z, S) plane. However, the thermodynamically stable strangelets do not correspond to the radius minimum. The minimum radius always appears at positive strangeness, while the stable radius may appear at negative strangeness for very small baryon numbers. For large baryon numbers, the stable radius is proportional to the cubic root of baryon numbers, but inversely proportional to the square root of the confinement parameter in the present model. If bulk strange quark matter is absolutely stable, the reduced size of strangelets is about 1 fm, which may be relevant for the analysis of the strangelet production and detection.

*E-mail address: gxpeng@ihep.ac.cn

1 Introduction

Strange quark matter (SQM) has been one of the hot topics in nuclear physics since Witten's conjecture [1] that SQM might be the true ground state of strong interactions. Lumps of SQM are customarily called strangelets [2], or for short, slets [3]. There are basically two kinds of slets: one is the ordinary slets without pairing [2, 4, 5, 6, 7, 8], the other is the color superconductivity slets [9, 3, 10]. The possible terrestrial production of slets has been studied in high energy heavy ion experiments, e.g., at the CERN SPS energies [11]. For a review on recent experimental searches of quark-gluon plasma at Brookhaven RHIC, see Ref. [12]. At high densities, quark matter may be the most favorite phase, and could thus exist in the core of compact stars [13]. Strange star collisions could release slets as part of the energetic cosmic rays, and some of the cosmic ray slets might be on the way to our Earth [14, 15]. The Alpha Magnetic Spectrometer (AMS-02) [16], which is planned to operate on the International Space Station, may offer the opportunity to detect these slets [17].

It is still an interesting open problem whether or not these cosmic ray slets incident on top of the Earth's atmosphere can reach to the ground or sea level. In fact, several exotic cosmic ray events with anomalously low charge-to-mass ratio have been observed at rather low altitudes [18, 19, 20]. In literature, one finds a number of possible scenarios of slet propagation which depends strongly on assumed size of slets. For example, the radius of slets used in [21] is different from that in [22, 23] by nearly an order of magnitude. Since the mean free path of a slet in the atmosphere is strongly dependent on its radius R_{slet}, as, for instance, in the simple law $\lambda = A_{\mathrm{air}} m_{\mathrm{N}} / [\pi (R_{\mathrm{slet}} + R_{\mathrm{air}})^2]$ where $m_{\mathrm{N}} \approx 939$ MeV is the nucleon mass, $A_{\mathrm{air}} \approx 14.5$ and $R_{\mathrm{air}} = 1.12 A_{\mathrm{air}}^{1/3} \approx 2.73$ fm are, respectively, the mean mass number and radius of the nucleus in the atmosphere, different radii led to significantly different conclusions.

Meanwhile, the charge property of slets is very important, as shown by Madsen *et al.* who found that the slets of low charge-to-mass ratio are favored in the ultra-high-energy

cosmic rays [24], and the color flavor locked (CFL) slets have charge $Z \approx 0.3A^{1/3}$ where A is the baryon number. Jaffe *et al.* also demonstrated that the slets with large baryon number have positive charges $Z \sim A^{1/3}$ [4]. In addition to these positively charged slets, negative charges are also possible for both ordinary [25] and CFL slets [3] in beta equilibrium. At the same time, the strangeness fraction is also an important factor to determine the stable configuration of slets [6].

Recently, we suggested a new quark mass scaling [26] based on the linear confinement, and the new model was applied to investigating the properties of slets in full beta equilibrium. In heavy ion collision experiments, however, the time scale is not enough for perfect beta equilibrium. Moreover, the charge/strangeness composition, and especially the size of slets, are quite important and useful to analyse possibility of production and detection of slets [21]. In this paper, therefore, we study the relevant properties of slets with the new quark mass scaling in [26], without imposing beta equilibrium, and with focus on the slet size. It is found that the mechanically stable radius of a slet with fixed baryon number and temperature is not a monotonic function of either charge Z or strangeness S. The radius has a minimum in the (Z, S) plane. However, the radius minimum does not correspond to the minimum of free energy. We determine the composition of thermodynamically stable slets by minimizing the free energy. For a large baryon number A, the corresponding slet radius is $R = [(3/4)^{1/3}/\sqrt{x_0 D}]A^{1/3}$, where $x_0 = 1.3278478$, and D is the confinement parameter in the present model. If SQM is absolutely stable, the reduced stable radius is $r_{\text{slet}} \equiv R/A^{1/3} \approx 1$ fm. In the conventional bag model, slets always contain strange quarks. In the present model, we find that very small slets tend to contain anti-strangeness, and the ratio of charge to baryon number increases.

This paper is organized as follow. In Sec. 2 we introduce the thermodynamic treatment with density and temperature dependent quark masses. The properties of strangelets related to the strangeness and electric charge at both zero and finite temperature are presented in Sec. 3. A summary is given in the final section 4.

2 Thermodynamics with density and temperature dependent quark masses

We start from the total free-particle thermodynamic potential density

$$\Omega = \sum_i \Omega_i(T, \mu_i, m_i, R), \tag{1}$$

where the summation index i goes over u, d, s quark flavors , T is the temperature, m_i and μ_i ($i = u, d, s$) are the corresponding quark masses and chemical potentials, and R is the slet radius. At finite temperature, we treat the anti-quarks as a whole with quarks. The contribution of the thermodynamic potential density from the density of state $n'_i(p, m_i, R)$ is given in the multi-expansion approach [27] as

$$
\begin{aligned}
\Omega_i &= -T \int_0^\infty \left\{ \ln \left[1 + e^{-(\sqrt{p^2+m_i^2}-\mu_i)/T} \right] \right. \\
&\quad \left. + \ln \left[1 + e^{-(\sqrt{p^2+m_i^2}+\mu_i)/T} \right] \right\} n'_i(p, m_i, R) \mathrm{d}p,
\end{aligned} \tag{2}
$$

where the density of state is

$$n'_i(p, m_i, R) = \frac{3}{\pi^2} \left\{ p^2 - \frac{3p}{2R} \arctan\left(\frac{m_i}{p}\right) + \frac{1}{R^2}\left[1 - \frac{3p}{2m_i}\arctan\left(\frac{m_i}{p}\right) \right] \right\}. \tag{3}$$

The three terms on the right are, respectively, the volume term, surface term [2, 4] and curvature term [28].

To include the confinement interaction between quarks, we treat the quark mass as density and temperature dependent, i.e. $m_i = m_i(n_\mathrm{b}, \mathrm{T})$, where $n_\mathrm{b} = \sum_i n_i/3$ with n_i ($i = u, d, s$) being the quark number densities. This means that the mass of quarks and antiquarks varies with state parameters in a medium. We can divide the quark mass into two parts: one is the current mass m_{i0}, the other is the interacting term m_I, i.e., $m_i = m_{i0} + m_\mathrm{I}$. In the present calculations, we take the quark current masses $m_{u0} = 5$ MeV, $m_{d0} = 10$ MeV and $m_{s0} = 120$ MeV, respectively. Because the strong interaction between quarks is a color interaction, m_I is common for all quark flavors. The key point is how to determine the interaction m_I.

In Ref. [29], the ansatz $m_{\mathrm{I}} = \frac{B_0}{3n_{\mathrm{b}}}[1 - (T/T_{\mathrm{c}})^2]$ was introduced. Because it caused an unreasonable temperature dependence of the slet radius, another term linear in temperature was added [8]. Based on the in-medium chiral condensates and linear confinement, we recently derived a new quark mass scaling, which can be expressed as [26]

$$m_i = m_{i0} + \frac{D}{n_{\mathrm{b}}^z}\left[1 - \frac{8T}{\lambda T_{\mathrm{c}}}\exp\left(-\lambda\frac{T_{\mathrm{c}}}{T}\right)\right], \tag{4}$$

where $\lambda = \mathrm{LambertW}(8) \approx 1.60581199632$ is a constant, $T_{\mathrm{c}} = 170$ MeV is the critical temperature. The exponent z was previously taken to be 1 [30, 31, 32]. In order to be consistent with the linear confinement, derivations based on the in-medium chiral condensates [33] showed that it is more reasonable to take $z = 1/3$ [34, 35, 36]. The confinement parameter D can be constrained to a very narrow range by stability arguments and we take $D^{1/2} = 156$ MeV [37].

The particle number density for each quark flavor can be derived by the following expression

$$n_i = -\frac{\partial\Omega}{\partial\mu_i}. \tag{5}$$

The pressure is

$$P = -\Omega - \frac{R}{3}\frac{\partial\Omega}{\partial R} + n_{\mathrm{b}}\sum_i\frac{\partial\Omega}{\partial m_i}\frac{\partial m_i}{\partial n_{\mathrm{b}}}, \tag{6}$$

where the last term is due to the density dependence of quark masses [37, 32]. The partial derivatives $\partial m_i/\partial n_{\mathrm{b}}$ in Eq. (6) can be easily obtained from the quark mass scaling in Eq. (4), i.e.,

$$\frac{\partial m_i}{\partial n_{\mathrm{b}}} = -\frac{zD}{n_{\mathrm{b}}^{z+1}}\left[1 - \frac{8T}{\lambda T_{\mathrm{c}}}\exp\left(-\lambda\frac{T_{\mathrm{c}}}{T}\right)\right] = -z\frac{m_{\mathrm{I}}}{n_{\mathrm{b}}}. \tag{7}$$

Accordingly the free energy density of the slets is

$$F = \Omega - \sum_i\mu_i\frac{\partial\Omega}{\partial\mu_i}. \tag{8}$$

5

At zero temperature, the relevant integrations can be carried out. The quark number densities in Eq. (5) become

$$n_i = \frac{\nu_i^3}{\pi^2} + \frac{9m_i^2}{4\pi^2 R}\left[(x_i^2 + 1)\arctan(x_i) - x_i\left(\frac{\pi}{2}x_i + 1\right)\right]$$
$$+ \frac{9m_i}{4\pi^2 R^2}\left[(x_i^2 + 1)\arctan(x_i) - x_i\left(\frac{3\pi}{2}x_i - 1\right)\right]. \tag{9}$$

where $\nu_i = \sqrt{\mu_i^2 - m_i^2}$ is the Fermi momentum of the quark flavor i and $x_i \equiv \nu_i/m_i$. The free energy density in Eq. (8) becomes the energy density

$$E = \sum_{i=u,d,s} \frac{3m_i^4}{8\pi^2}\left\{\left[x\left(2x_i^2 + 1\right)\sqrt{x^2 + 1} - \ln\left(x + \sqrt{x^2 + 1}\right)\right]\right.$$
$$+ \frac{2}{m_i R}\left[\pi - x_i\sqrt{x_i^2 + 1} - \mathrm{arcsh}(x_i) - 2(x_i^2 + 1)^{3/2}\mathrm{arccot}(x_i)\right]$$
$$\left.+ \frac{2}{(m_i R)^2}\left[\pi + x_i\sqrt{x_i^2 + 1} + \mathrm{arcsh}(x_i) - 2(x_i^2 + 1)^{3/2}\mathrm{arccot}(x_i)\right]\right\}. \tag{10}$$

And the pressure in Eq. (6) becomes

$$P = \sum_{i=u,d,s} \frac{m_i^4}{8\pi^2}\left\{x_i(2x_i^2 - 3)\sqrt{x_i^2 + 1} + 3\mathrm{arcsh}(x_i) - 12z\frac{m_\mathrm{I}}{m_i}\left[x_i\sqrt{x_i^2 + 1} - \mathrm{arcsh}(x_i)\right]\right.$$
$$+ \frac{2}{m_i R}\left[3\pi\sqrt{x_i^2 + 1} - 2\pi - 4x_i\sqrt{x_i^2 + 1} + 2\mathrm{sh}^{-1}(x_i) - 2(x_i^2 + 1)^{3/2}\mathrm{arccot}(x_i)\right.$$
$$\left.- 9z\frac{m_\mathrm{I}}{m_i}\left(x_i\sqrt{x_i^2 + 1} + \pi - \pi\sqrt{x_i^2 + 1} - \mathrm{sh}^{-1}x_i\right)\right]$$
$$\frac{1}{(m_i R)^2}\left[\pi(3\sqrt{x_i^2 + 1} - 2) - 2\mathrm{arcsh}(x_i) - 2(x_i^2 + 1)^{3/2}\mathrm{arccot}(x_i)\right.$$
$$- 3z\frac{m_\mathrm{I}}{m_i}\left(4\pi - 3\pi\sqrt{x_i^2 + 1} + 2x_i\sqrt{x_i^2 + 1}\right.$$
$$\left.\left.\left. + 4\mathrm{arcsh}(x_i) - 2(x_i^2 + 1)^{3/2}\mathrm{arccot}(x_i)\right)\right]\right\}. \tag{11}$$

In the above Eqs. (9), (10), and (11), $\mathrm{arcsh}(x_i) \equiv \ln(x + \sqrt{x^2 + 1})$ is the inverse hyperbolic sine, $\arctan(x_i)$ and $\mathrm{arccot}(x_i)$ are the inverse tangent and cotangent functions. Please note, the interaction part of the quark mass scaling, i.e., the second term on the right hand side of Eq. (4), simply gives $m_\mathrm{I} = D/n_\mathrm{b}^z$ at zero temperature.

3 Properties of strangelets

Thanks to the pioneer works of Witten and Jaffe *et al.* [1, 2], we have known a lot about slets. The properties of slets away from beta equilibrium were also investigated by mode filling in Ref. [6] where the authors checked possible strong and weak hadronic decays (also multiple hadron decays) and found that slets stable against strong decays were most likely highly negatively charged. Mode filling studies are very important to show shell effect [38], but it is difficult for large baryon numbers. Therefore, a multi-expansion liquid-drop model was developed [28]. Similar studies were done by He *et al.* at finite temperature [5] and Zhang *et al.* with their suggested quark mass scaling (QMDTD) [39]. In this section, we apply our newly derived quark mass scaling in Eq. (4) to investigate the properties of slets.

In relativistic heavy ion experiments, a slet, if formed, has no time to be in perfect beta equilibrium. We therefore regard it as a mixture of u, d and s quarks. Given three conserved quantities, i.e., the baryon number A, strangeness S and electric charge Z, we have the following equations:

$$A = \frac{1}{3}(N_u + N_d + N_s), \tag{12}$$

$$Z = \frac{2}{3}N_u - \frac{1}{3}N_d - \frac{1}{3}N_s, \tag{13}$$

$$S = N_s, \tag{14}$$

where N_u, N_d, N_s are the number of u, d, and s quarks. For the mechanically stable slets, the internal pressure must be zero, i.e.

$$P = 0. \tag{15}$$

We define the charge to baryon number ratio and strangeness fraction as $f_z = Z/A$ and $f_s = S/A = N_s/A$. Two different linear combinations of the Eqs. (12) and (13) give $N_u = A + Z$ and $N_d + N_s = 2A - Z$. We then easily get

$$f_z = N_u/A - 1, \tag{16}$$

7

$$f_s = 3 - (N_u + N_d)/A. \tag{17}$$

Because we consider only $0 < N_u < 3A$ and $0 < N_d < 3A$, the possible range for f_z and f_s are $-1 \le f_z \le 2$ and $-3 \le f_s \le 3$. With a view to the relation $f_z + f_s = 2 - N_d/A$, we have $-1 - f_z \le f_s \le 2 - f_z$ if f_z is fixed, and we can write $-1 - f_s \le f_z \le 2 - f_s$ if f_z is given.
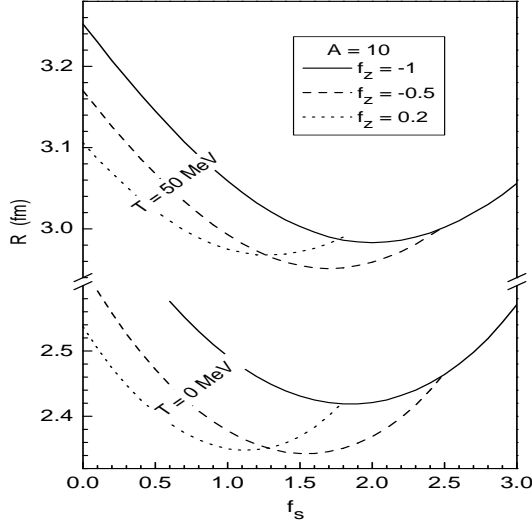

Figure 1: The mechanically stable radii of a strangelet with baryon number $A = 10$ at temperature $T = 0$ and 50 MeV is shown as functions of its strangeness fraction f_s for given ratios of charge to baryon number. A minimum is reached on each curve.
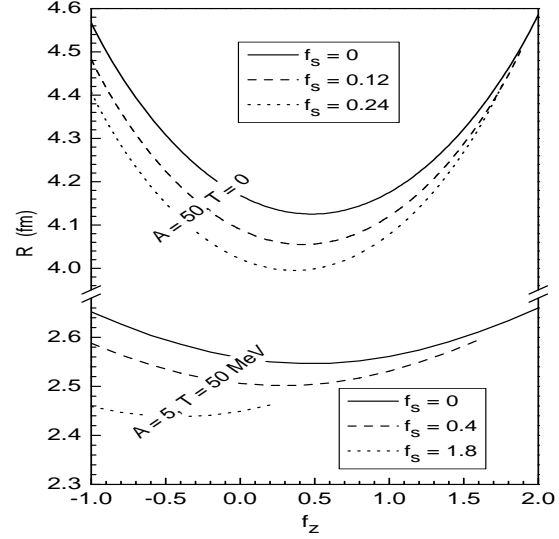
Figure 2: The radius of a strangelet as functions of the charge to baryon number ratio at different given strangeness fraction. The up part is for $A = 50$ and $T = 0$, while the down part is for $A = 5$ and $T = 50$ MeV. One can also find a minimum on every curve.

For a definite set of values for A, f_z, f_s, one can easily get the quark numbers by $N_u = A(1 + f_z), N_d = A(2 - f_z - f_s), N_s = Af_s$. If we give an arbitrary value to the radius R, then the slet volume is $V = (4/3)\pi R^3$, and the density is $n_b = A/V = 3A/(4\pi R^3)$. At a given temperature, the quark density and temperature dependent mass can be accordingly calculated from Eq. (4). The respective chemical potential μ_i $(i = u, d, s)$ can then be obtained by solving $n_i = 3N_i/(4\pi R^3)$ with the n_i expression in Eq. (5). The pressure and

free energy density are calculated by Eqs. (6) and (8), respectively. We numerically vary R until the pressure becomes zero when the mechanically stable radius is reached.

At the fixed baryon number $A = 10$, we give the slet radius as a function of the strangeness fraction f_s at $T = 0$ (the down part) and $T = 50$ MeV (the up part) in Fig. 1. The solid, dashed, and dotted curves correspond, respectively, to the charge to baryon number ratio $f_z = -1$, -0.5, and 0.2. It is obvious that the radius is not a monotonic function of strangeness. The position of the minimum radius depends on electric charge fraction. It is also natural that the radius increases with increasing temperature.

Similarly in Fig. 2, we show the radius of strangelets as functions of the charge fraction. The variation of the radius with respect to electric charge is not monotonic at the fixed strangeness. The curves are also parabolas as in the above Fig. 1. Generally, the minimum radius will appear at the middle position of the region $(-1, 2 - f_s)$.

For comparison, we have also done calculations with the conventional bag model, with the results shown in Fig. 3. The left (right) panel shows the radius with respect to strangeness (charge) fraction for $A = 10$ at zero temperature. One also finds a minimum on each curve. Therefore, it is safe to conclude that the radius of slets is not monotonic. Instead, it has a minimum with respect to the charge and strangeness. This minimum is the smallest radius for a given pair of baryon number and temperature. However, the smallest radius does not necessarily correspond to the thermodynamically stable slets obtained by minimizing the free energy.

Now we investigate the thermodynamically stable radius of a slet with given baryon number at fixed temperature. In order to understand how the stable radius appears analytically, we may fall back on the fundamental differentiation equality of thermodynamics, i.e.,

$$dF = SdT - PdV + \sum_i \mu_i dN_i. \tag{18}$$

At fixed temperature T and $P = 0$, we have

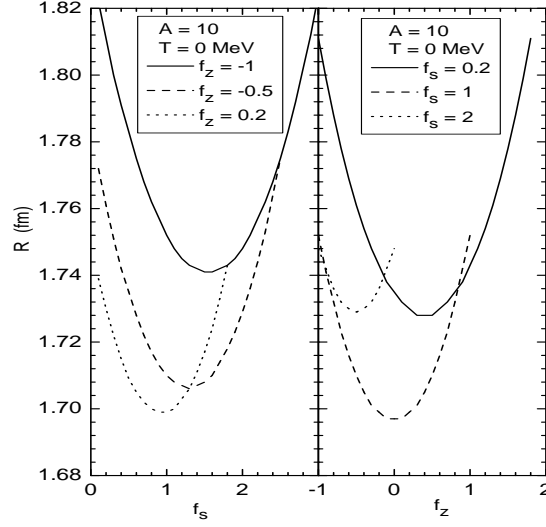$$dF = \sum_i \mu_i dN_i. \tag{19}$$

9

Figure 3: The strangeness (left panel) and charge (right panel) dependence of the strangelet radius in the conventional bag model. The relevant parameters are $A = 10$, $T = 0$ and $B^{1/4} = 180$ MeV. A minimum is also obviously reached on every curve.

If A and Z are fixed, we obtain naturally,

$$\frac{\partial(F/A)}{\partial f_s} = \mu_s - \mu_d. \tag{20}$$

Similarly, with fixed A and N_s we get

$$\frac{\partial(F/A)}{\partial f_z} = \mu_u - \mu_d. \tag{21}$$

From Eqs. (20) and (21), we draw an important conclusion that the minimum of the free energy per baryon occur when $\mu_d = \mu_s$ with fixed A and Z in the F/A-f_s panel, and when $\mu_u = \mu_d$ with fixed A and S in the F/A-f_z panel. Therefore, we can get the stablest radius for a slet with given A and T by requiring the condition

$$\mu_u = \mu_d = \mu_s, \tag{22}$$

i.e., in this case only one chemical potential is independent. The only independent one can be determined by solving the equation

$$\frac{1}{3}(n_u + n_d + n_s) = n_{\rm b} \quad \text{with} \quad n_{\rm b} = \frac{3A}{4\pi R^3} \tag{23}$$
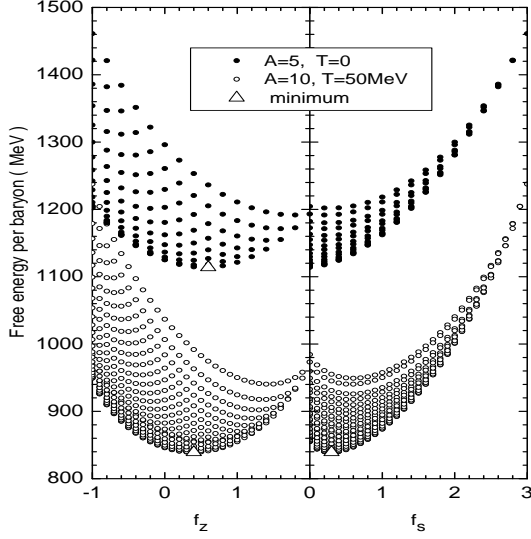
10

Figure 4: The free energy of strangelets versus the ratio of charge to baryon number (left panel) and the strangeness fraction (right panel) for the two cases: $A = 5, T = 0$ and $A = 10, T = 50$.
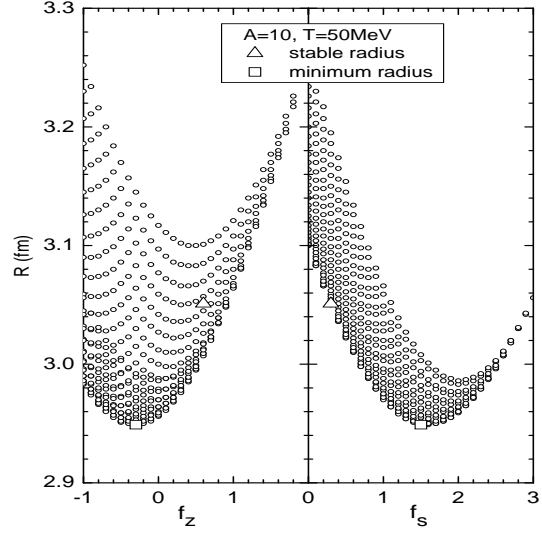
Figure 5: Comparison of the smallest radius (the square) and the thermodynamically stable radius (the triangle) in the R-f_z plane (left panel) and in the R-f_s (right panel) for $A = 10$ and $T = 50$ MeV.

for an arbitrary radius. We finally vary the radius R so that the zero pressure condition is satisfied, and accordingly we obtain the stable radius.

As mentioned in the introduction section, the size of slets is very important for analyzing their propagation and detection. Therefore, let's pay special attention to the case of zero temperature and try to derive an approximate expression for the radius.

Because $\nu_i = \sqrt{\mu_i^2 - m_i^2}$, Eq. (22) is equivalent to

$$\sqrt{\nu_u^2 + m_u^2} = \sqrt{\nu_d^2 + m_d^2} = \sqrt{\nu_s^2 + m_s^2} \equiv \mu^*, \tag{24}$$

where we have used μ^* as the common effective chemical potential. This means $\nu_i = \sqrt{\mu*^2 - m_i^2}$, or $x_i = \sqrt{(\mu^*/m_i)^2 - 1}$ where $i = u, d,$ or s quarks. Substituting these into the n_i given in Eq. (5) or Eq. (9) at zero temperature, then substituting into Eq. (23), we obtain an equation which contains the common chemical potential μ^* and the radius R. Similarly substitution into the pressure expression in Eq. (6) or (11), we get another equation

11

of μ^* and R. The radius is then obtained by solving the two equations of μ^* and R.

Because the surface and curvature terms can be regarded as a perturbation to the volume terms, and also because the interaction part of the quark mass is greater than the quark current masses $(m_{\mathrm{I}} > m_{i0})$, we can ignore the finite-size effect and iso-spin effect to derive a first-order approximation for the radius. In this case, we have $\nu_u = \nu_d = \nu_s \equiv \nu_0$ and $x_u = x_d = x_s \equiv x_0$, and the zero pressure condition becomes

$$x_0(2x_0^2 - 3)\sqrt{x_0^2 + 1} + 3\mathrm{arcsh}(x_0) - 12z\left[x_0\sqrt{x_0^2 + 1} - \mathrm{arcsh}(x_0)\right]. \tag{25}$$

The positive solution of this equation is $x_0 \approx 1.3278478$ (The trivial solution $x_0 = 0$ and the non-physical solution $x_0 = -1.3278478$ were discarded). At the same time, Eqs. (9) and (23) at the same order approximation gives $n_i = \nu_i^3/\pi^2 = n_{\mathrm{b}} = 3A/(4\pi R^3)$. Combining this with $x_0 = \nu_0/m_{\mathrm{I}} = (\pi^2 n_{\mathrm{b}})^{1/3}/(D/n_{\mathrm{b}}^{1/3}) = (\pi n_{\mathrm{b}})^{2/3}/D$, or $n_{\mathrm{b}} = (x_0 D)^{3/2}/\pi$, we immediately have

$$R = \frac{(3/4)^{1/3}}{\sqrt{x_0 D}} A^{1/3} \equiv r_{\mathrm{slet}} A^{1/3}. \tag{26}$$

For the chosen value $D = (156 \text{ MeV})^2$, the reduced slet radius is

$$r_{\mathrm{slet}} = R/A^{1/3} = (3/4)^{1/3}\Big/ \sqrt{x_0 D} = 0.9973 \text{ fm}. \tag{27}$$

This value is smaller than that of normal nuclei, but bigger than the recent value (~ 0.94 fm) [40] from the conventional bag model calculations. Equation (26) shows that the slet radius is inversely proportional to the square root of the confinement parameter D. If one uses a bigger D value, then the slet radius can be very small. In that case, however, SQM will not be absolutely stable.

It should be emphasized that the expression for the slet radius in Eq. (26) is only the lowest order approximation because it was obtained by ignoring the finite size effect and isospin dependence (quark mass difference). The actual size is a a little bit bigger, from 1 fm (for large baryon numbers) to about 1.2 fm (for small baryon numbers). So Eq. (26) is only accurate for slets with large baryon numbers. In the following we continue to present the numerical results.
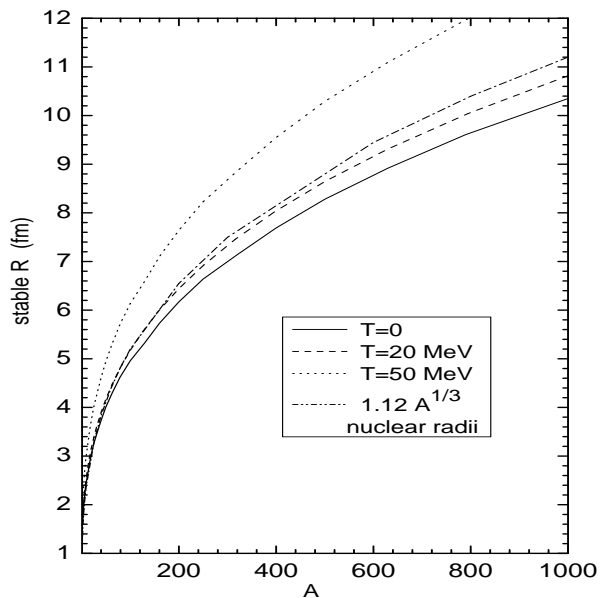
Figure 6: The baryon number dependence of the strangelet radius at temperature $T = 0$ (solid curve), 20 MeV (dashed curve), and 50 MeV (dotted curve). The dash-dotted curve is for the ordinary nuclei radius $R = 1.12A^{1/3}$ fm.

We show all possible slets with positive strangeness in Fig. 4. The full dots are for $A = 5$ and $T = 0$, while the open circles are for $A = 10$ and $T = 50$ MeV. The left (right) panel gives the distribution of the free energy per baryon on the f_z (f_s) axis. The triangle denotes the minimum of the free energy per baryon, i.e., the most stable slets. For a given pair of A and T, therefore, we have two special values for the radius of a slet via varying the strangeness fraction f_s and the charge to baryon number ratio f_z: the first one is obtained by minimizing the radius itself, and thus is the smallest radius, while the second one is obtained by minimizing the free energy of the system, and is thus the thermodynamically stable radius. The obvious difference between the smallest radius (square) and the stable radius (triangle) is compared in Fig. 5, where the smallest radius is 2.95 fm for $A = 10$ and $T = 50$ MeV while the stable radius is 3.05 fm.

The baryon number dependence of the stable slet radius is shown in Fig. 6 at temperature $T = 0$ (solid line), 20 MeV (dashed line), and 50 MeV (dotted line). To compare, the normal

13

nuclear radii have also been shown with a dash-dotted line. We see that the radii of slets are comparable with those of ordinary nuclei.
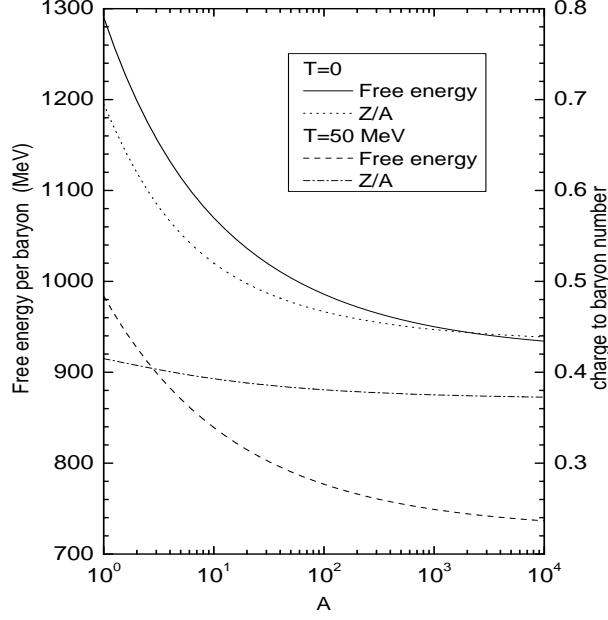

Figure 7: The free energy per baryon (left axis) and the charge to baryon number Z/A (right axis) of stable strangelets vary with the baryon number A. They are generally decreasing functions. With increasing temperature, the decreasing speed goes down, and Z/A is very flat at high temperature.
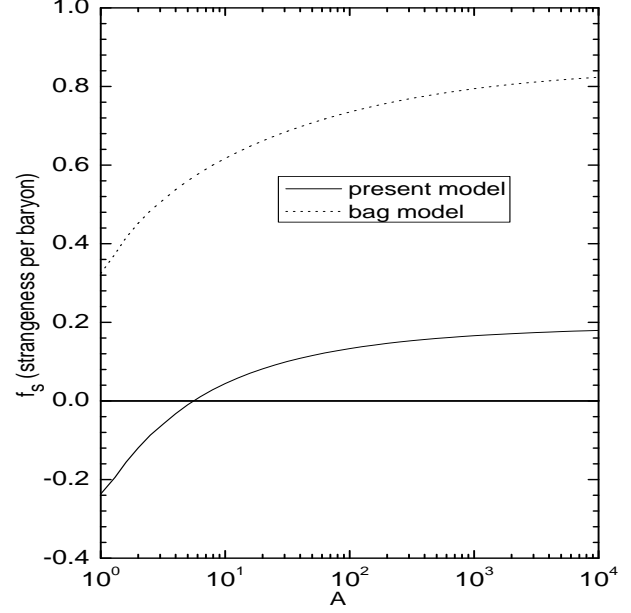
Figure 8: The strangeness per baryon for stable strangelets as a function of the baryon number at zero temperature. For very small baryon numbers, the strangeness fraction in the present model (solid curve) becomes negative, while that in the bag model (dotted curve) is always positive.

Fig. 7 gives the free energy per baryon and the charge to baryon number ratio of stable slets as a function of the baryon number. It is seen that the free energy per baryon decreases with both increasing temperature and baryon number. When the temperature is as high as up to 50 MeV, the dash-dotted line for charge to baryon number becomes very flat. The smaller the baryon number, the more important the influence of temperature on the charge to baryon number.

In Fig. 8, we show the strangeness fraction f_s, with a solid line, as a function of the

baryon number at zero temperature. The striking feature is that the strangeness fraction becomes negative for very small baryon numbers. In fact, this feature has already been seen in the up part of the right panel in Fig. 4 where the minimum of the free energy was not reached at positive strangeness. For comparison, we also give, in the same figure with a dotted line, the results from the conventional bag model in which the quark masses are constant and the strangeness fraction is always positive. In the present model, however, the quark masses are density and temperature dependent. Therefore, the strangeness fraction becomes negative for very small baryon numbers, and the charge to baryon number ratio becomes bigger than that in the bag model.

4 Summary

We have studied the properties of strangelets in a new quark mass scaling without imposing beta equilibrium. It is found that the radius of strangelets is not a monotonic increasing or decreasing function of either electric charge or strangeness. By varying the strangeness and charge for a given pair of baryon number and temperature, we have calculated the smallest radius and thermodynamically stable radius, and have shown that they are generally different. The stable radii of strangelets can be calculated approximately by the law $R = r_{\text{slet}} A^{1/3}$. If SQM is absolutely stable, the reduced radius of strangelets is $r_{\text{slet}} = (3/4)^{1/3}/\sqrt{x_0 D} \sim 1$ fm. The smallest radius appears always at positive strangeness. However, the stable strangelets could have negative strangeness fraction for very small baryon numbers. This means that very small strangelets may contain anti-strangeness.

The present study is still model-dependent. Many problems, e.g., how the anti-strangeness content influences the stability and detectability of strangelets in heavy ion experiments, to what extent the behavior of the radius can be used to analyze the production and detection of strangelets, etc, need to be further explored.

Acknowledgements

References

[1] Witten E 1984 *Phys. Rev. D* **30** 272

[2] Farhi E and Jaffe R L 1984 *Phys. Rev. D* **30** 2379

[3] Peng G X, Wen X J, and Chen Y D 2006 *Phys. Lett. B* **633** 314

[4] Berger M S and Jaffe R L 1987 *Phys. Rev. C* **35** 213

[5] He Y B, Gao C S, Li X Q, Chao W Q 1996 *Phys. Rev. C* **53** 1903

[6] Schaffner-Bielich J, Greiner C, Diener C, and Stoecker H 1997 *Phys. Rev. C* **55** 3038

[7] Madsen J 2000 *Phys. Rev. Lett.* **85** 4687

[8] Zhang Y, Su R K, Ying S Q, and Wang P 2001 *Europhys. Lett.* **53** 361

[9] Madsen J 2001 *Phys. Rev. Lett.* **87** 172003

[10] Alford M G, Rajagopal K, Reddy S, and Steiner A W 2006, *Phys. Rev. D* **73** 114016

[11] Lourenco C 2002 *Nucl. Phys. A* **698** 13c

[12] Weiner M 2006 *Int. J. Mod. Phys. E* **15** 37

[13] Peng G X 2005 *Europhys. Lett.* **72** 69

[14] Finch E 2006 *J. Phys. G* **32** S251

[15] Monreal B 2007 *J. High Energy Phys.* **0702** 077

[16] Sandweiss J 2004 *J. Phys. G* **30** S51

[17] Cheng K S, Usov V V 2006 *Phys. Rev. D* **74** 127303

[18] Saito T, Hatano Y, and Fukada Y 1990 *Phys. Rev. Lett.* **65** 2094
    Kasuya M *et al* 1993 *Phys. Rev. D* **47** 2153

[19] Ichinura M *et al* 1993 *Nuovo Cimento* A **106** 843

[20] Price P B *et al* 1978 *Phys. Rev.* D **18** 1382
    Saito T 1995 *Proc. 24th Internat. Cosmic Ray Conf. (Rome)* Vol. **I** p. 890

[21] Wilk G and Wlodarczyk 1996 *J. Phys. G* **22** L105

[22] Capdeville J N *et al* 1995 *Proc. 24th Internat. Cosmic Ray Conf. (Rome)* Vol. **I** p. 910

[23] Miyamura O *et al* 1995 *Proc. 24th Internat. Cosmic Ray Conf. (Rome)* Vol. **I** p. 890

[24] Madsen J and Larsen J M 2003 *Phys. Rev. Lett.* **90** 121102

[25] Peng G X, Chiang H C, Ning P Z, Zou B S 1999 *Phys. Rev. C* **59** 3452

[26] Wen X J, Zhong X H, Peng G X, Shen P N, and Ning P Z 2005 *Phys. Rev. C* **72** 015204

[27] Balian R and Bloch C 1970 *Ann. Phys* **60** 401

[28] Madsen J 1993 *Phys. Rev. Lett.* **70** 391
    Madsen J 1993 *Phys. Rev. D* **47** 5156 Madsen J 1994 *Phys. Rev. D* **50** 3328

[29] Zhang Y and Su R K 2002 *Phys. Rev. C* **65** 035202

[30] Fowler G N, Raha S, and Weiner R M 1981 *Z. Phys. C* **9** 271

[31] Chakrabarty S, Raha S, and Sinha B 1989 *Phys. Lett. B* **229** 112
    Chakrabarty S, *Phys. Rev. D* bf 43 627

[32] Benvenuto O G and G. Lugones G 1995 *Phys. Rev. D* **51** 1989

17

[33] Peng G X 2005 *Nucl. Phys. A* **747** 75

[34] Peng G X, Chiang H C, Yang J J, Li L, and Liu B 2000 *Phys. Rev. C* **61** 015201

Peng G X, Lombardo U, Loewe L, and Chiang H C 2002 *Phys. Lett. B* **548** 189

[35] Lugones G and Horvath J E 2003 *Int. J. Mod. Phys. D* **12** 495

[36] Zheng X P, Liu X W, Kang M, and Yang S H 2004 *Phys. Rev. C* **70** 015803

[37] Peng G X, Chiang H C, and Ning P Z 2000 *Phys. Rev. C* **62** 025801

[38] Gilson E P and Jaffe R L 1993 *Phys. Rev. Lett.* **71** 332

[39] Zhang Y and Su R K 2003 *Phys. Rev. C* **67** 015202

[40] Wu F, Xu R X, and Ma B Q 2007 *J. Phys. G* **34** 597